Acta Cryst. (1982). A**38**, 725–729

A Measurement of Charge Asphericity in Iron Metal

BY SHIGERU OHBA AND YOSHIHIKO SAITO

Department of Chemistry, Faculty of Science and Technology, Keio University, 3-14-1 Hiyoshi, Kohoku-ku, Yokohama 223, Japan

AND YASUTOSHI NODA

Department of Materials Science, Faculty of Engineering, Tohoku University, Aramaki Aoba, Sendai 980, Japan

(*Received* 22 *December* 1981; *accepted* 12 *May* 1982)

Abstract

Electron-density distribution in metallic iron has been determined based on the reflection data measured up to $\sin\theta/\lambda = 1{\cdot}36$ Å^{-1} with Mo $K\alpha$ radiation using a spherical specimen of 0·186 (6) mm in diameter. Fe is cubic, $Im3m$, $a = 2{\cdot}8652$ (1) Å, $V = 23{\cdot}522$ (3) Å^3, $Z = 2$, μ(Mo $K\alpha$) = 30·35 mm^{-1} ($T = 297$ K). Final R was 0·007 for the 37 unique reflections, the internal agreement factor for the equivalent reflections being 0·013 for the 527 observed reflections. In the difference synthesis a positive peak of 0·7 (1) e Å^{-3} was found in the [111] direction at 0·32 (1) Å from the iron nucleus and a trough of −0·6 (1) Å^{-3} was found in the [100] direction at 0·54 (1) Å from the nucleus. Charge asphericity in iron metal, presumably due to the 3*d* electrons in t_{2g} orbitals, is essentially the same as that of the other 3*d* b.c.c. metals, V and Cr.

Introduction

Crystal structure of V, Cr and Fe metals is body-centered cubic (b.c.c.) at room temperature and under normal pressure. Since Weiss & DeMarco (1965) detected the charge asphericity for vanadium metal, aspherical 3*d* electron distribution in these b.c.c. metals has been studied experimentally as well as theoretically [see Table 1 of Wakoh & Kubo (1980) and Table 11 of Weiss & Mazzone (1981)]. Charge asphericity has been estimated only by the intensity ratios of the paired reflections which have the same $\sin\theta/\lambda$ value such as $F^2(442)/F^2(600)$. Recently, charge asphericity in the crystals of vanadium and chromium metals was detected on the difference syntheses (Ohba, Sato & Saito, 1981; Ohba, Saito & Wakoh, 1982). As an extension of this study, metallic iron has been examined.

Experimental

α-Iron single crystals were prepared by chemical transport reaction (Schäfer, 1964). A block of iron cut from a rod with a nominal purity of 99·99% (purchased from Johnson & Matthey Co., London) was vacuum sealed in a quartz ampoule (length 100 mm, internal diameter 8 mm) with iodine as a transport agent at a concentration of 2 kg m^{-3}. The temperatures of the ampoule were set at 1053 K for growth chamber and at 1073 K for evaporation chamber. After one week, single crystals were obtained as rectangular parallelepipeds with well-developed {100} faces ranging up to about 0·5 mm edge length. The crystals were annealed at 773 K in a stream of dry hydrogen for 10 h in order to remove the non-metallic impurities (Hörz, 1976).

Single crystals of pure iron are so soft that they are easily cut with a thin knife. It was found on the oscillation photographs that the spots of reflections from the crystal specimen considerably expanded after grinding. With caution against the strain on a crystal in grinding, a spherical crystal 0·186 (6) mm in diameter was prepared by hand with a piece of sandpaper under a stereomicroscope and its surface was etched with an ethanol solution of nitric acid. Intensity measurement was performed at 297 K on a Rigaku automated four-circle diffractometer equipped with a graphite-plate monochromator and a pulse-height analyser. Integrated intensity measurement with the use of Ag $K\alpha$ radiation was attempted, but failed because it was impossible to observe the whole intensity of the reflexions for the following reason: The reflection peak extended on both sides of the ω scan axis and owing to the white X-rays it also fell into a tail in the high-angle side of the θ–2θ scan axis. Intensity measurements were performed with Mo $K\alpha$ radiation ($\lambda = 0{\cdot}7107$ Å). Peak profiles of 020, 060 and 262 are shown in Fig. 1. The solid and broken lines indicate the profiles for ω and θ–2θ scan modes, respectively, as a function of ω. The integrated intensity obtained by the ω scan mode was greater than that obtained by the θ–2θ scan mode for the low-angle reflections owing to mosaicity of the crystal. Low-angle reflections ($2\theta \leq 70°$) were measured by the ω scan technique with a scan width of 8°. A scan width of 3° was adequate for the ω scan

0567-7394/82/050725-05$01.00

mode but the scan width of 8° was selected because the $|F_o|$'s increased by a few percent when the scan width was increased from 3 to 8°. The peak half-width for 020 is 0·36°, indicating that the crystal specimen used was not so poor. Intensity zero level is also drawn in Fig. 1. There was no difficulty in extracting the peak intensity from the background. For example, the peak intensity of 020 was 11 000 counts s^{-1}. The background of the lower- and higher-angle side of the 8° ω scan were 8·7 and 5·3 counts s^{-1}, respectively. For the high-angle reflections such as 262 [2θ(Mo $K\alpha$) = 110°], the peak splitting by the $K\alpha_1$ and $K\alpha_2$ components could not be covered by the ω scan technique, so the θ–2θ scan mode was adopted in the range $100 < 2\theta \leq 150°$ with a scan width of $(3 + \tan\theta)°$. The reflections in the range $70 < 2\theta \leq 100°$ were measured by both scan techniques and the larger integrated intensity data were adopted. The intensities obtained by the two types of scan mode are compared in Fig. 2. Other experimental conditions as well as crystal data are listed in Table 1. 527 reflections in a hemisphere of reciprocal space were measured, which contained 37 independent reflections. The integrated intensities of 011 were measured with the variation of azimuthal angles, Ψ, around the scattering vector, the largest variation of $|F(011)|$ being 7·4%. These data were also used for the refinement. The unit-cell constant was determined to be 2·8652 (1) Å based on the 51 2θ values in the range from 71 to 81°, measured on a diffractometer with Ag $K\alpha_1$ radiation (λ = 0·559408 Å).

Refinement

Correction was made for Lorentz and polarization effects. Thermal diffuse scattering was also corrected by the program *TDS2* (Stevens, 1974) using the elastic-constant data of Rayne & Chandrasekhar (1961). The largest correction factor was 0·955 for $|F(730)|$.* Absorption correction for a spherical crystal with μr(Mo $K\alpha$) = 2·82 was performed by the Lagrange interpolation method with the transmission factor taken from *International Tables for X-ray Crystallography* (1959). The absorption correction factor for $|F_o|$ was in the range from 2·9 to 5·4. The mean path length of each reflection, which was used for the secondary-extinction correction, was calculated as $\bar{T} = \{-r/A(\mu r)\}\{[A(\mu r + \Delta\mu r) - A(\mu r)]/\Delta\mu r\}$, where A is the transmission factor, μ is the linear absorption coefficient, and r is the radius of the crystal specimen. $\Delta\mu r$ was set to 0·01. It is noted that the approximation for the spherical crystal, $\bar{T} = -\{\log A\}/\mu$, proposed by Coppens & Hamilton (1970) can be used only when the μr value is smaller than about 0·5 as described in their paper. Scale and isotropic thermal parameters were refined by the full-matrix least-squares program *RADIEL* (Coppens, Guru Row, Leung, Stevens, Becker & Yang, 1979). The function minimized was $R_w(F) = [\sum w(|F_o| - |F_c|)^2/\sum w|F_o|^2]^{1/2}$, where the weight was assigned as $w^{-1} = [\sigma(|F_o|)]^2 + (0{\cdot}015|F_o|)^2$. Introduction of an isotropic secondary-extinction correction parameter (Zachariasen, 1967) decreased the $R(F)$ factor ($= \sum ||F_o| - |F_c||/\sum |F_o|$) from 0·039 to 0·014. The smallest extinction factor (F_o^2/F_c^2) was 0·74 for 110. Anisotropic secondary-extinction correction (Coppens & Hamilton, 1970) could not reduce the R factors significantly. In the case of heavy absorption of incident X-rays, the Borrmann effect must be considered in the secondary-extinction correction (Zachariasen, 1968). Fortunately, the mean radius of a perfect-crystal domain was estimated to be 2×10^{-6} mm, which is so small that the Borrmann effect can be neglected. The final $R(F)$ was 0·014 and $R_w(F)$ was 0·018 for the 564 observed reflections. Figure of merit, $S = [\sum w(|F_o| - |F_c|)^2/(No - Np)]^{1/2}$, was 1·14. After averaging equivalent reflections, $R(F)$ and $R_w(F)$ became 0·007 and 0·008 for the 37 unique

* TDS correction factors have been deposited (see footnote below).

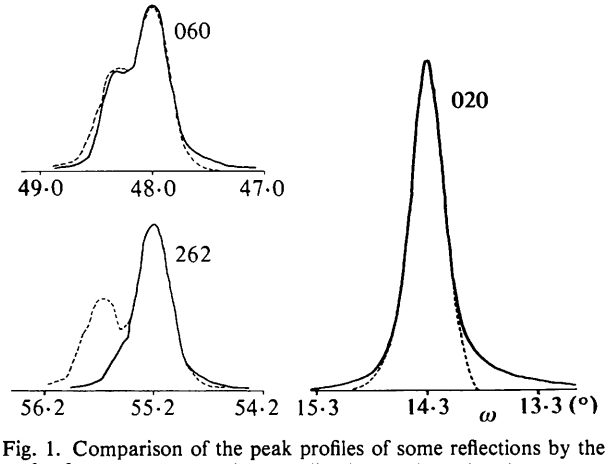

Fig. 1. Comparison of the peak profiles of some reflections by the θ–2θ scan technique (broken lines) and those by the ω scan technique (solid lines) as a function of ω.

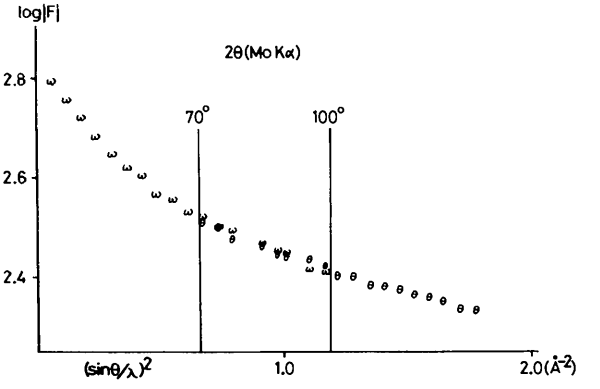

Fig. 2. A plot of $\log|F|$ as a function of $(\sin\theta/\lambda)^2$ with the intensities obtained by the θ–2θ scan (θ) and by the ω scan (ω).

Table 1. *Crystal data and experimental conditions*

Fe (at 297 K)	
Cubic, $a = 2{\cdot}8652$ (1) Å, $V = 23{\cdot}522$ (3) Å^3	
Space group $Im3m$, $Z = 2$, μ(Mo $K\alpha$) = 30·35 mm^{-1}	
$C_{11} = 0{\cdot}231$, $C_{12} = 0{\cdot}1354$, $C_{44} = 0{\cdot}1178$ N μm^{-2} (Rayne & Chandrasekhar, 1961)	
Diameter of crystal specimen	0·186 (6) mm
Radiation	Mo $K\alpha$ ($\lambda = 0{\cdot}7107$ Å)
Monochromator	Graphite plate
Collimator	0·5 mm ○
Detector aperture	8·6 mm ○ (2·1°)
$(\sin\theta/\lambda)_{max}$ of the observed reflections	1·36 Å^{-1}
Scan mode	ω scan ($2\theta \le 100°$)
	θ–2θ scan ($70 < 2\theta \le 150°$)
Scan speed	2° min^{-1} in θ
Scan width	8° (ω scan)
	(3 + tan θ)° (θ–2θ scan)
Maximum number of repetitions	4
Criterion to terminate repetition	$\sigma(\|F\|)/\|F\| \le 0{\cdot}005$
Number of reflections measured	527
Number of non-zero reflections	527
Number of independent reflections	37

reflections, respectively.* The internal agreement factor of each independent reflection, $\sum \|\|F_o\| - \langle\|F_o\|\rangle\| / \sum \|F_o\|$, ranged from 0·005 to 0·018. The total internal agreement factor was 0·013 for the 564 observed reflections. The scattering factor of the neutral Fe atom and the anomalous dispersion correction terms were taken from *International Tables for X-ray Crystallography* (1974). The observed mean-square amplitude of the atomic thermal vibration, U, is 0·00507 (2) Å^2. The corresponding Debye characteristic temperature is 400 K, which falls in the middle of the values found in the literature, ranging from 355 to 467 K (*International Tables for X-ray Crystallography*, 1962).

* Lists of structure factors and TDS correction factors have been deposited with the British Library Lending Division as Supplementary Publication No. SUP 36915 (3 pp.). Copies may be obtained through The Executive Secretary, International Union of Crystallography, 5 Abbey Square, Chester CH1 2HU, England.

Results and discussion

Intensity ratios of the paired reflections, having the same $\sin\theta/\lambda$ values, are listed in Table 2. Compared with the experimental results using plate-like crystals (DeMarco & Weiss, 1965; Diana & Mazzone, 1974) and that of the present work obtained by the spherical specimen, the ratio $F^2(330)/F^2(411)$ agreed well. Concerning the 442–600 pair, the ratio obtained by a plate-like crystal is larger than that of the present study, as was found for vanadium metal (see Table 1 of Ohba, Sato & Saito, 1981). In view of the accuracy of the experiments, the difference in the results obtained by the two experimental techniques may be meaningless. To show the accuracy of the present study, all of the observed structure factors of equivalent reflections for the 330–411 pair are shown in Fig. 3. $|F(330)|$'s are marked with open circles and $|F(411)|$'s with crosses. The mean values of $|F(330)|$ and $|F(411)|$ are shown by the horizontal lines. We are discussing the charge asphericity based on the width formed by these two lines. Variation of the structure factor within the equivalent reflections is greater than the difference between the mean values of the independent reflections. One of the origins of the systematic errors in $|F_o|$ seems to be the non-sphericity in the shape of the crystal specimen, which was described in some detail previously (Ohba, Sato & Saito, 1981). The theoretical ratios derived by band calculation (DeCicco & Kitz, 1967; Wakoh & Yamashita, 1971; Duff & Das, 1971; Callaway & Wang, 1977) are less than those of the experimental works. By the use of orbital-dependent potentials instead of orbital-independent ones, theoretical asphericity for iron metal is expected to increase as in the case of V and Cr metals (Wakoh & Kubo, 1980; Ohba, Saito & Wakoh, 1982). Philips & Weiss (1972) performed a model calculation employing expanded $3d$ radial wave functions with the e_g orbitals expanded considerably more than the t_{2g} orbitals. Their calculated ratios are in good agreement with the experimental values.

Table 2. *Experimental and theoretical ratios of the integrated intensities of the reflection pairs for iron metal*

E.s.d.'s of the experimental ratios are shown in parentheses.

	Experimental			Theoretical				
F^2/F^2*	Present study	DeMarco & Weiss (1965)	Diana & Mazzone (1974)	DeCicco & Kitz (1967)	Wakoh & Yamashita (1971)	Duff & Das (1971)	Callaway & Wang (1977)	Phillips & Weiss (1972)
330/411	1·020 (14)	1·023 (5)	1·020	1·006	1·006	1·015	1·004	1·028
431/510	1·018 (10)			1·009				
433/530	1·015 (12)			1·005				
442/600	1·032 (17)	1·050 (10)		1·012	1·012			1·054
532/611	1·018 (11)			1·008				

* The ratio of the paired reflections $h_1k_1l_1$ and $h_2k_2l_2$ is defined at $F^2(h_1k_1l_1)/F^2(h_2k_2l_2)$, where the value of $h_1^4 + k_1^4 + l_1^4$ is always selected to be less than that of $h_2^4 + k_2^4 + l_2^4$.

Difference electron densities were calculated based on the 37 unique reflections (maximum $\sin\theta/\lambda$ is 1·36 Å^{-1}). The section of the (110) plane through the Fe nucleus is shown in Fig. 4. General features of the difference synthesis are essentially the same as that of the chromium metal (Ohba, Saito & Wakoh, 1982). A positive peak of 0·7 (1) e Å^{-3} in height is located on the [111] axis at 0·32 Å from the Fe nucleus. On the other hand, a trough of −0·6 (1) e Å^{-3} is found on the [100] axis at 0·54 Å from the nucleus.* The observed charge asphericity indicates that the 3*d* electron population of the t_{2g} orbitals is greater than $\frac{3}{5}$ (a spherically symmetric charge density). By the method of Weiss & DeMarco (1965) the t_{2g} orbital population was estimated to be 64·8 (1·4)% from the integrated intensity ratios of the first five reflection pairs. The corresponding value of the V and Cr metals was 66·6 (2·8) and 67·0 (2·3)%, respectively (Ohba, Sato & Saito, 1981; Ohba, Saito & Wakoh, 1982), where the electron configuration was assumed as $(3d)^n(4s)^1$ (n = 4, 5 and 7 for V, Cr and Fe metals, respectively) and the form factors $\langle j_0\rangle_{3d}$ and $\langle j_4\rangle_{3d}$ of the neutral atoms were employed (*International Tables for X-ray Crystallography*, 1974). The number of *d* electrons which contributes to the charge asphericity can be written as $(5\alpha - 3)n/2$, where α is the population of the t_{2g} orbitals and n is the total number of 3*d* electrons. The number of aspherical *d* electrons are 0·66, 0·88 and 0·84 for V, Cr and Fe, respectively. It is noteworthy that the asphericity of the spin density in metallic iron, observed by magnetic scattering using polarized neutron radiation, is inverse to that of the charge density: excess magnetic-moment density was observed on the [100] axis at 0·47 Å from the nucleus and a deficiency on the [111] axis at 0·48 Å from the nucleus (Shull & Yamada, 1962). An electron-population analysis considering the spin moment was performed by DeMarco & Weiss (1965) for metallic iron. By combining neutron and X-ray results and assuming the electron configuration as $(3d)^{7\cdot2}$ and the number of unpaired spins as 2·05, they estimated the orbital population of the metallic iron as follows: 5·0 electrons (70% of the total 3*d* electrons) occupy the t_{2g} orbitals, of which 3·0 electrons are in the spin-up band; in e_g orbitals the number of spin-up electrons is 1·6 of 2·2.

* The standard deviation assigned to the deformation density was estimated from the errors in the observed structure factors and an error in the scale factor (Toriumi & Saito, 1978).

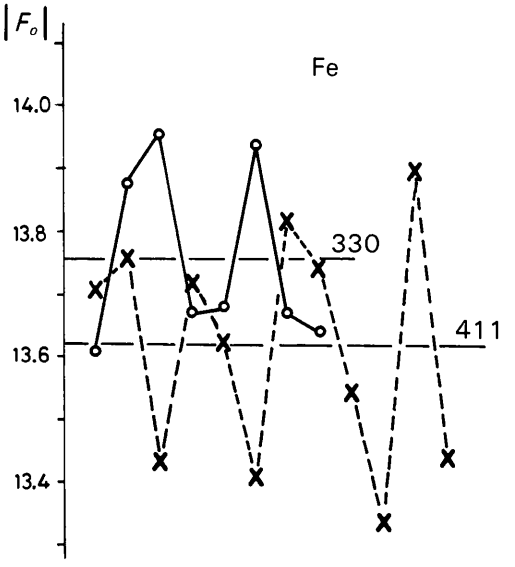

Fig. 3. Observed structure factors of equivalent reflections for the 330–411 pair.

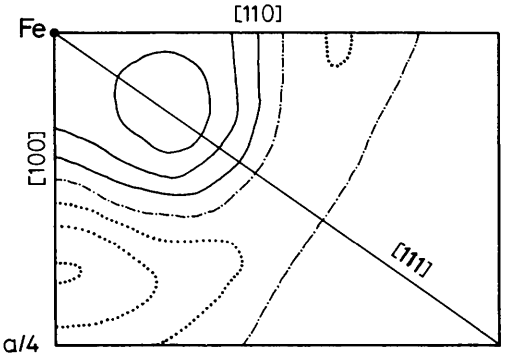

Fig. 4. A section of the difference synthesis through the Fe nucleus and parallel to the (110) plane. Contours are drawn at intervals of 0·2 e Å^{-3}. Negative contours are dotted, zero contours chain-dotted.

The authors are grateful to Dr S. Takagi of The Research Institute for Iron, Steel and Other Metals, Tohoku University for annealing the crystals in a stream of dry hydrogen. They are also indebted to The Institute for Solid State Physics, The University of Tokyo for the use of the X-ray four-circle diffractometer and the FACOM M-160F computer.

References

CALLAWAY, J. & WANG, C. S. (1977). *Phys. Rev. B*, **16**, 2095–2105.

COPPENS, P., GURU ROW, T. N., LEUNG, P., STEVENS, E. D., BECKER, P. J. & YANG, Y. W. (1979). *Acta Cryst.* A**35**, 63–72.

COPPENS, P. & HAMILTON, W. C. (1970). *Acta Cryst.* A**26**, 71–83.

DECICCO, P. D. & KITZ, A. (1967). *Phys. Rev.* **162**, 486–491.

DEMARCO, J. J. & WEISS, R. J. (1965). *Phys. Lett.* **18**, 92–93.

DIANA, M. & MAZZONE, G. (1974). *Phys. Rev. B*, **9**, 3898–3904.

DUFF, K. J. & DAS, T. P. (1971). *Phys. Rev. B*, **3**, 2294–2306.

HÖRZ, G. (1976). *Gase und Kohlenstoff in Metallen.* Edited by E. FROMM & E. GEBHART, pp. 84–201. Berlin: Springer-Verlag.
International Tables for X-ray Crystallography (1959). Vol. II, p. 300. Birmingham: Kynoch Press.
International Tables for X-ray Crystallography (1962). Vol. III, p. 235. Birmingham: Kynoch Press.
International Tables for X-ray Crystallography (1974). Vol. IV, p. 78, pp. 112–116, p. 149. Birmingham: Kynoch Press.
OHBA, S., SAITO, Y. & WAKOH, S. (1982). *Acta Cryst.* A**38**, 103–108.
OHBA, S., SATO, S. & SAITO, Y. (1981). *Acta Cryst.* A**37**, 697–701.
PHILLIPS, W. C. & WEISS, R. J. (1972). *Phys. Rev. B*, **6**, 4213–4219.
RAYNE, J. A. & CHANDRASEKHAR, B. S. (1961). *Phys. Rev.* **122**, 1714–1716.
SCHÄFER, H. (1964). *Chemical Transport Reactions* (translated by H. FRANKFORT), pp. 35–98. NY, London: Academic Press.
SHULL, C. G. & YAMADA, Y. (1962). *J. Phys. Soc. Jpn*, **17**, Suppl. B-III, 1–6.
STEVENS, E. D. (1974). *Acta Cryst.* A**30**, 184–189.
TORIUMI, K. & SAITO, Y. (1978). *Acta Cryst.* B**34**, 3149–3156.
WAKOH, S. & KUBO, Y. (1980). *J. Phys. F*, **10**, 2707–2715.
WAKOH, S. & YAMASHITA, J. (1971). *J. Phys. Soc. Jpn*, **30**, 422–427.
WEISS, R. J. & DEMARCO, J. J. (1965). *Phys. Rev.* **140**, A1223–1225.
WEISS, R. J. & MAZZONE, G. (1981). *J. Appl. Cryst.* **14**, 401–416.
ZACHARIASEN, W. H. (1967). *Acta Cryst.* **23**, 558–564.
ZACHARIASEN, W. H. (1968). *Acta Cryst.* A**24**, 421–424.

Acta Cryst. (1982). A**38**, 729–733

Anharmonic Thermal Vibrations and Atomic Potentials in Lead Fluoride (β-PbF_2) as a Function of Temperature

BY HEINZ SCHULZ, E. PERENTHALER AND U. H. ZUCKER

Max-Planck-Institut für Festkörperforschung, Heisenbergstrasse 1, *D*-7 *Stuttgart* 80, *Federal Republic of Germany*

(*Received* 1 *April* 1981; *accepted* 12 *May* 1982)

Abstract

Bragg intensities of β-PbF_2 (with the cubic fluorite structure) have been measured in the step-scan mode up to $\sin\theta/\lambda = 1{\cdot}17$ Å^{-1} at 295, 461 and 625 K by X-ray diffraction: $a = 5{\cdot}925\,(2)$, $5{\cdot}952\,(2)$, $5{\cdot}982\,(4)$ Å, respectively; $R = 0{\cdot}013$ for 103 reflections, 0·015 for 103 reflections, 0·018 for 106 reflections, respectively. The intensities were used for the refinement of anharmonic temperature factors up to third order for F^- and up to sixth order for Pb^{2+}. The temperature-factor formalism was based on the Gram–Charlier expansion. The probability density function (p.d.f.) of the F^- and Pb^{2+} ions were calculated from the coefficients of the anharmonic temperature factors. The p.d.f. maps gave clear evidence that the Pb^{2+} ions do not carry out isotropic thermal motion. The atomic potentials of the Pb^{2+} ions (derived from the p.d.f. maps) indicate that the thermal motion of the excited Pb^{2+} ions is strongly influenced by the repulsion terms along the Pb^{2+}–F^- bonds. The F^- ions carry out their largest thermal vibrations along $\langle 111 \rangle$ towards the centre of the elementary cell.

Introduction

β-PbF_2 crystallizes in the fluorite structure type. It exhibits a high F^- conductivity at medium temperatures. Furthermore, the F^- ions show pronounced anharmonic thermal vibrations along the body diagonals. Similar observations have been made for several other fluorides. The anharmonic part of the thermal motion of the F^- ions have been partly described by so-called split atoms or by a third-order temperature coefficient. Anharmonic thermal vibrations and ionic conductivity are closely related to each other. A discussion of these effects and a literature survey are given by Koto, Schulz & Huggins (1981). Only harmonic temperature factors have been applied to the lead ions in all of these investigations. Owing to the high point symmetry of the Pb^{2+} atomic position only an isotropic temperature factor is allowed for the harmonic model. If anharmonic thermal vibrations are considered, temperature factors (temperature tensors) of order four and six are allowed. The coefficients of these tensors can be determined by least-squares refinements of Bragg intensities. A discussion of the

0567-7394/82/050729-05$01.00